Mem. S.A.It. Suppl. Vol. 13, 104

Memorie della
Supplementi

Modeling magnetohydrodynamics and non-equilibrium SoHO/UVCS line emission of CME shocks

P.Pagano[1,2,3], J.C. Raymond[3], and F.Reale[1,2]

[1] Dipartimento di Scienze Fisiche ed Astronomiche, Sezione di Astronomia, Università di Palermo, Piazza del Parlamento 1, 90134 Palermo, Italy
[2] INAF - Osservatorio Astronomico di Palermo, Piazza del Parlamento 1, 90134 Palermo, Italy
[3] Harvard-Smithsonian Center for Astrophysics, 60 Garden Street, Cambridge, MA 02138

Abstract. The Coronal Mass Ejections are plasma clouds expelled from the Sun into the interplanetary medium. We study the propagation of shock waves in the solar corona generated during Coronal Mass Ejections by means of a numerical multi-dimensional MHD model. The model describes the MHD evolution of a compressible plasma in an ambient magnetic field including tensor thermal conduction, radiative losses as main physical effects. We use the MHD version of the FLASH parallel hydrodynamic code with adaptive mesh refinement, originally developed at the University of Chicago USA). The code is highly modular and made efficiently parallel with the Message Passing Interface library. We analyze the diagnostic signatures of shock fronts generated by supersonic CME fragments detectable with the UltraViolet Coronagraphic Spectrometer on board the SoHO mission. To this aim we perform 3D MHD simulations of the shock propagation for the time it takes to cross the UVCS slit positioned at a distance of a few solar radii from the solar surface. In the presence of highly effective thermal conduction the simulation takes 200000 time steps to cover 1000 s of evolution. Considering a 3-D domain of 256x256x512 grid cells this kind of simulations requires thousands of hours of computer time and therefore high performance computing (HPC) systems. The simulations were run on the CINECA IBM/SP5 HPC cluster within the INAF/CINECA agreement. We show simulation results and some implications for UVCS observations.

Key words. Sun: coronal mass ejections (CMEs); Magnetohydrodynamics (MHD); Sun: corona

1. Introduction

A Coronal Mass Ejection (CME) is a sudden and fast ejection of material from the solar corona. It envolves usually about $\sim 10^{15}$ g of coronal plasma expelled at the speed of ~ 500 km/s, though several faster CMEs (up to $\sim$ 2000 km/s) have been observed. Strong shock waves are expected to develop from fast CMEs. According to the most popular idea about the structure of CMEs, an expanding magnetic flux rope propagates in the solar corona and this leads to the creation of the CME leading edge and to the creation of shocks, as well. It is

widely accepted that the front side halo CMEs are strongly correlated with geomagnetic disturbances (Brueckner et al. 1998; Cane et al. 2000; Gopalswamy et al. 2000; Webb et al. 2000; Zhang et al. 2003). Thus, the detection of CME related shocks is a crucial topic in space weather research. However, it is also a difficult problem, because it cannot be confirmed from white light images alone. Sharp edges in white light images have been taken as evidence of shocks at the CME leading edge, but it is impossible to prove that they are shocks without the support of deeper diagnostics.

The UltraViolet Coronograph Spectrometer (UVCS) (Kohl et al. 1995) on board the Solar and Heliospheric Observatory (SoHO) (Domingo & Poland 1988) gave a strong impulse to this research topic. This is a spectrometer whose field of view is a slit and its images are maps of intensity of radiation as function of wavelength and position along the slit. The spectral analysis gives a deep diagnostics on the density, temperature, velocity and abundances of the observed plasma and UVCS is tuned to clearly measure O VI and H lines. (Ciaravella et al. 2006) pointed out the correlation between the shocks and several spectral properties of the post-shock emission. Overall, they found that the shock emission is comparable or weaker than the background coronal emission. The O VI 1032 Å line is usually broad, but its intensity does not increase. Instead the Si XII brightens significantly and it is common that the intensity of the line doubles, and the Ly α fades. This general description is based on several studies made on different CME events which reached similar conclusion. For instance, broad O VI lines and more intense Si XII line have been observed in 2000 June 28 (Ciaravella et al. 2005), 2000 September 12 (Suleiman et al. 2005) and 2000 October 24 (Ciaravella et al. 2006) event. In the shock related to the CME event on June 11, 1998 the derived compression and ionization appear modest with respect to the inferred shock strength (Raymond et al. 2000). Because of our purposes, any attempt to model observables in shock wave propagation cannot neglect that the highly dynamic plasma can be easily in Non Equilibrium of Ionization (NEI) (Spadaro et al. 1994), since the time scales are too short to allow the ionization state of the plasma to relax.

The aim of this work is to find unambiguous spectral shock signatures, and to provide a guide for the interpretation of general features that could appear in UVCS observations. Our approach is to model in detail and diagnose the propagation of a shock wave generated from a supersonic fragment of a CME in the magnetized corona. We use a numerical Magnetohydrodynamic (MHD) model (Pagano et al. 2007) to describe the MHD evolution and from the result we compute the plasma emission for the O VI and Si XII lines which are diagnostically important in UVCS observations of shock waves including the effects of NEI.

In Section 2 we describe our model, Sec.3 includes the results discussed in Sec.4.

2. The model

We use a full MHD model of the solar corona tuned to investigate the coronal emission visible from UVCS during a shock wave propagation. We model a supersonic CME core fragment moving upward in a magnetohydrostatic solar corona. During its propagation, the fast cloud generates a series of shock waves, and we study how the waves perturb the quiet corona. To this aim, we need to model the evolution of both the plasma and the magnetic field and, to compute emission, also of the ion abundances.

We consider the solar gravity, the radiative losses (e.g. (Raymond & Smith 1977), a phenomenological coronal heating term and the field-oriented thermal conduction (Spitzer 1962) as important physical effects. The full MHD equation we solve are:

$$\frac{\partial \rho}{\partial t} + \boldsymbol{\nabla} \cdot (\rho \boldsymbol{v}) = 0 \tag{1}$$

$$\frac{\partial \rho \boldsymbol{v}}{\partial t} + \boldsymbol{\nabla} \cdot (\rho \boldsymbol{v}\boldsymbol{v}) = -\nabla p + \frac{(\boldsymbol{\nabla} \times \boldsymbol{B}) \times \boldsymbol{B}}{4\pi} + \rho \boldsymbol{g} \tag{2}$$

$$\frac{\partial u}{\partial t} + \boldsymbol{\nabla} \cdot [(u+p)\boldsymbol{v}] = \rho \boldsymbol{g} \cdot \boldsymbol{v} - n^2 P(T) + H_0 - \boldsymbol{\nabla} \cdot \boldsymbol{F_c} \tag{3}$$

$$\frac{\partial \boldsymbol{B}}{\partial t} = \boldsymbol{\nabla} \times (\boldsymbol{v} \times \boldsymbol{B}) \quad (4)$$

$$u = \frac{1}{2}\rho v^2 + E \quad (5)$$

$$p = (\gamma - 1)E \quad (6)$$

with the constraint given by:

$$\nabla \cdot \boldsymbol{B} = 0 \quad (7)$$

where t is the time, ρ is the density, n the number density, p the thermal pressure, T the temperature ($T_e = T_p = T_i$ in this model), $\boldsymbol{v}$ the plasma flow speed, u the total energy (internal energy E plus kinetic), $\boldsymbol{g}$ the gravity acceleration, $\boldsymbol{F_c}$ is the conductive flux according to (Spitzer 1962) and corrected for the saturation effect (Cowie & McKee 1977), $P(T)$ the radiative losses per unit emission measure (Raymond & Smith 1977), $H_0 = n_0^2 P(T_0)$ is a constant heating term whose only role is to keep steady the unperturbed corona by balancing exactly its radiative losses, with $n_0(\boldsymbol{r}) = n(\boldsymbol{r}, t = 0)$ and $T_0 = T(t = 0)$ (Pagano et al. 2007). We do not include plasma resistivity effects, which can be considered globally negligible on large scales in the solar corona.

We solve numerically the set of the ideal full MHD equations with the MHD module of the advanced parallel FLASH code, basically developed by the ASC / Alliance Center for Astrophysical Thermonuclear Flashes in Chicago (Fryxell et al. 2000), with Adaptive Mesh Refinement (PARAMESH, (MacNeice et al. 2000)). We include the FLASH module for the anisotropic thermal conduction (Spitzer 1962) implemented by (Pagano et al. 2007), and improved for the saturation effects by (Orlando et al. 2005)

We compute the ionization state of the plasma from the history and distribution of $\boldsymbol{v}$, n_e and T obtained with the MHD model. This is done asynchronously of the MHD computations. The ionization state is computed considering the lagrangian transport of ions, and the ionization/recombination processes, i.e. we are not assuming ionization equilibrium during the simulation. The evolution of the electron density and of the plasma motion throughout the domain are taken from the MHD model results (sampled every 25 s).

The intensity of the lines is computed as the sum of the collisional (I_c) and radiative (I_r) contribution:

$$I = I_c(n_e, n_i^Z, T) + I_r(n_i^Z, T, \boldsymbol{v}) \quad (8)$$

We model the evolution of a dense cloud moving upward supersonically in the outer coronal atmosphere as shown in Fig. 1. The

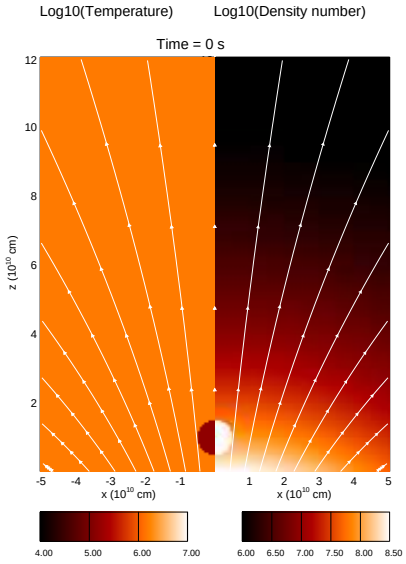

Fig. 1. Initial condition of the model. The panel shows a section at $y = 0$ of the temperature and density number spatial distributions. The the magnetic field lines are also shown (white lines).

center of the cloud (i.e. the CME fragment) is initially positioned at $0.15 R_\odot$ above the photosphere and has an upward initial velocity of 1000 km/s. It is 10 times denser than the surroundings, but in pressure equilibrium with them (i.e. colder than the surroundings atmosphere). The atmosphere is isothermal at 1.5 MK and stratified by gravity in such a way to have $n = 10^8 cm^{-3}$ at the initial CME fragment center height. The background magnetic field is modeled as a dipole laying in the center of the Sun and seen from the central axis and such

intense to have $|\boldsymbol{B}| \sim 0.5$ G at the cloud center height.

The simulation is performed in a 3-D cartesian domain (x,y,z) that is $(8\times8\times16)\times10^{10}$ cm large, for the duration needed by the shock to propagate well above $2R_\odot$ which is the height where we put a hypothetical UVCS observations and is $\sim 1000s$. The simulation ran on the IBM/SP5 cluster of the CINECA hosted in Bologna, and took about 2 years of computational time, which actually meant 11 days on 64 processors.

3. Results

In Fig. 2 the density and the temperature of the plasma after 1000 s of evolution are shown. Shock fronts depart from the upper part of the high speed cloud. Here we address the shock evolution only, and not the cloud evolution. The cloud continuously shocks the surrounding medium, since its speed remains faster than the sound speed (at least during the time of our simulation), it cools down during the motion because of the radiative losses and its core becomes thermally unstable.

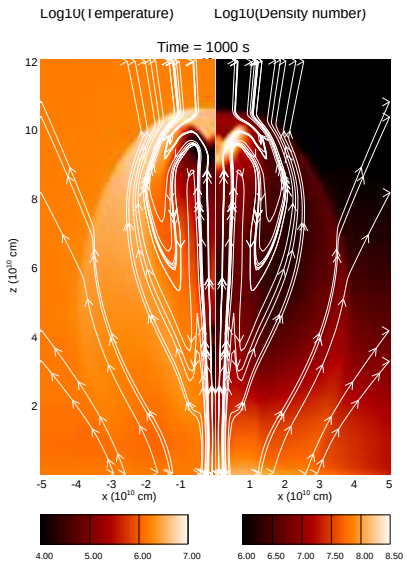

Fig. 2. As in Fig. 1, but at $t = 1000$ s in the reference simulation.

The shock propagates radially from the cloud. After 1000 s of evolution the cloud has reached the height of $\sim 2.5R_\odot$ and the produced shock edge has traveled $\sim 0.4R_\odot$ from the originating cloud.

The cloud velocity remains superalfvénic and the magnetic field is shocked as well. For this reason the post-shock magnetic field tends to be parallel to the shock front. The magnetic field pressure is negligible with respect to the plasma compression in the outer solar corona, but the magnetic field orientation influences the thermal properties of the shock and, as consequence, the ionization state. Since the shocked magnetic field is parallel to the shock front which is hotter than the surrounding atmosphere, the thermal conduction toward preshock regions is ineffective and the shocked plasma does not cool down. The shock heats the plasma, the ionization is enhanced and the ionization state changes. Immediately behind the shock the plasma is far from the ionization equilibrium at the shock temperature, and the ionization equilibrium is approached farther from the shock front, where the temperature has been no longer changing much and the plasma is slowly relaxing.

We apply our general radiation model to O VI and Si XII lines, that are important for the CME shock front diagnostics. Fig. 3 shows the evolution of the line intensity across the UVCS slit computed from the full MHD simulation and considering non-equilibrium of ionization. The intensity jump across the shock is sharper in the Si XII line than in the O VI line. Our model shows that the shocked plasma is far from ionization equilibrium; in fact, the heating time due to the shock is much shorter than the ionization equilibrium time and there is not enough time for the ionization state to change as soon as the shock has reached the plasma.

For diagnostic purposes, we focus the analysis at a characteristic height for the UVCS observations and for shock formation (Raymond et al. 2003), i.e. $2R_\odot$. The front of the bow shock begins to cross the UVCS slit field of view at ~ 675 s. UVCS detects first the upper and fastest part of this front and later the flanks. The shock strength decreases in time during the crossing of the UVCS slit field of

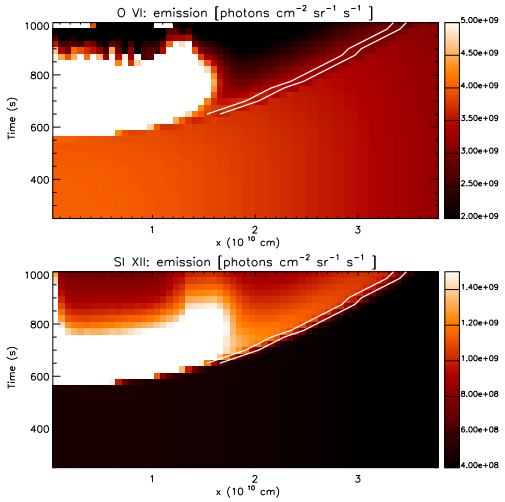

Fig. 3. Evolution of the emission of O VI (upper panel) and Si XII (lower panel) expected along an UVCS slit positioned at $2R_\odot$ integrated along the line of sight. The evolution is sampled every 25 s. The white lines mark the shock edge.

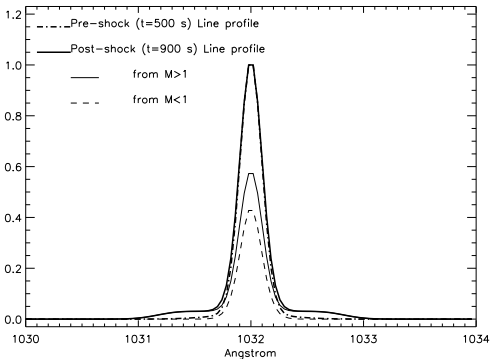

Fig. 4. Line profile of the O VI line synthesized from our reference model if observed as a limb CME at $t \sim 500$ s (point-dashed thick line) and at $t \sim 900$ s (solid thick line), i.e. before and after the shock crossed the UVCS field of view, respectively. The emission is averaged on time bins of 150 s and on space bins of 9' along the UVCS slit through which the CME is observed. The profile is normalized to the peak. We also show the two components which combine to form the line at $t \sim 900$: the one emitted by the shocked plasma ($\mathcal{M} > 1$, solid thin line) and the one emitted by the unshocked plasma ($\mathcal{M} < 1$, dashed thin line).

view and at t=700 s the plasma is accelerated to $\sim$ 500 km/s because of the shock and to $\sim$ 250 km/s at $t = 1000$ s. Since the radiative part of the Si XII is negligible, the total intensity of the post-shock line emission jumps significantly and relatively to the strength of the shock. As a consequence, the Si XII line clearly brightens, while the O VI line does not, as (Ciaravella et al. 2006) pointed out.

To further investigate the observational constraints for the shock properties we show here the line profile of the O VI lines synthesized from our reference model. This line is analyzed in detail by (Mancuso et al. 2002) who indicate shock diagnostics from UVCS observations. Here we try to provide further insight to that analysis, but our synthesis of the line profile is very general and could be applied also to the Si XII line after tuning the appropriate parameters.

We take into account the thermal broadening of the line and the Doppler shift due to the plasma motion projected along the line of sight, but not the instrumental broadening. To approach a realistic UVCS observation we average the spectrum over time bins of 150 s and over space bins of 9', mimicking a limb CME.

In Fig. 4 we plot the profile of the O VI line for the reference model as if it were observed as a limb CME before and after the shock passed the UVCS slit, i.e. expelled perpendicularly to the Sun-Earth radius. After the shock the central part of the line has not changed because it is emitted by that part of the plasma never involved in the shock passage. Evidence of the passage of the shock across the UVCS slit can instead be found in the wings of the later line. They are more prominent than in the quiet line, because of the line shift due to the line of sight component of the shock velocity. The resulting line profile is the sum of the emission contribution from pre-shock plasma and post-shock plasma. The un-shocked plasma emits only a narrow component (Fig. 4, $\mathcal{M} < 1$ line), while superposition of the lines emitted by the shocked plasma gives both a central component and sig-

nificant wings. These two emission contributions merge in a two component line. The first is a narrow and bright component, the sharp peak emitted by the unshocked corona and by the shocked plasma that moves perpendicularly to the line of sight; the second component is due to the shocked plasma that has a significant component of the velocity parallel to the line of sight, so that it emits thermally broadened lines centered far from 1032Å. (Mancuso et al. 2002) indeed observed a similar line profile and concluded that a shock was crossing the field of view of the UVCS slit during the observation. We argue that a two component line profile, as shown in Fig. 4, may in general be a signature of the presence of a shock.

4. Discussion and conclusions

In this work we study the shock fronts departing from supersonic CME fragments with detailed MHD modeling. We address the diagnostics obtainable with UVCS observations, which have been widely analyzed in this framework, and in particular the O VI and Si XII emission lines. As a result, we are able to explain most of the spectral signatures of the shocks revealed by the observations, and we step forward to predict more shock properties.

We have chosen a case where the shock front originating from a CME fragment 10 times denser than the surrounding 1.5 MK magnetized corona expelled at a speed of 1000 km/s. The ambient magnetic field is a large scale dipole. We have computed the emission in the selected lines and derived the line profiles with a detailed radiation model including the radiative and collisional contributions and the effects of non-equilibrium of ionization.

We find that some of the distinctive shock features detectable in O VI and Si XII lines arise from the relative brightness of the collisional and radiative contributions in the unperturbed corona. Since, the radiative contribution is actually negligible for Si XII, but important for O VI, the intensity jump across the shock is sharper in the Si XII line than in the O VI line.

When we observe the shock propagating from a limb CME we expect to observe a profile of the O VI line consisting on two distinct overlapping contributions. The unperturbed plasma that lies along the line of sight emits a narrow line and the shocked plasma emits a wider line. This combination is the kind of line shape that (Raymond et al. 2000) and (Mancuso et al. 2002) observed during the CME events. They used the double component line profile as signature of the shock. In our simulation we get the same line profile shape after the shock passage. Therefore we confirm that this spectral feature is a reliable signature of the shock presence.

Acknowledgements. They acknowledge support for this work from Agenzia Spaziale Italiana (contract I/035/05/0), Istituto Nazionale di Astrofisica and Ministero dell'Università e Ricerca. P. Pagano's stay at the Center for Astrophysics was supported by NASA grant NNG06GG78G to the Smithsonian Astrophysical Observatory. The calculations were performed on the IBM/SP5 machine at CINECA (Bologna, Italy). Part of the simulations were performed within a key-project approved in the INAF/CINECA agreement 2006-2007. The software used in this work was in part developed by the DOE-supported ASC / Alliance Center for Astrophysical Thermonuclear Flashes at the University of Chicago, using modules for thermal conduction and optically thin radiation built at the Osservatorio Astronomico di Palermo. CHIANTI is a collaborative project involving the NRL (USA), RAL (UK), MSSL (UK), the Universities of Florence (Italy) and Cambridge (UK), and George Mason University (USA).

References

Brueckner, G. E., Delaboudiniere, J.-P., Howard, R. A., et al. 1998, Geophys. Res. Lett., 25, 3019

Cane, H. V., Richardson, I. G., & Cyr, O. C. S. 2000, Geophys. Res. Lett., 27, 3591

Ciaravella, A., Raymond, J. C., & Kahler, S. W. 2006, ApJ, 652, 774

Ciaravella, A., Raymond, J. C., Kahler, S. W., Vourlidas, A., & Li, J. 2005, ApJ, 621, 1121

Cowie, L. L. & McKee, C. F. 1977, ApJ, 211, 135

Domingo, V. & Poland, A. I. 1988, SOHO: an observatory to study the solar interior and the solar atmosphere, Tech. rep.

Fryxell, B., Olson, K., Ricker, P., et al. 2000, ApJS, 131, 273

Gopalswamy, N., Lara, A., Lepping, R. P., et al. 2000, Geophys. Res. Lett., 27, 145
Kohl, J. L., Esser, R., Gardner, L. D., et al. 1995, Sol. Phys., 162, 313
MacNeice, P., Olson, K. M., Mobarry, C., de Fainchtein, R., & Packer, C. 2000, Computer Physics Communications, 126, 330
Mancuso, S., Raymond, J. C., Kohl, J., et al. 2002, A&A, 383, 267
Orlando, S., Peres, G., Reale, F., et al. 2005, A&A, 444, 505
Pagano, P., Reale, F., Orlando, S., & Peres, G. 2007, A&A, 464, 753
Raymond, J. C., Ciaravella, A., Dobrzycka, D., et al. 2003, ApJ, 597, 1106
Raymond, J. C. & Smith, B. W. 1977, ApJS, 35, 419
Raymond, J. C., Thompson, B. J., St. Cyr, O. C., et al. 2000, Geophys. Res. Lett., 27, 1439
Spadaro, D., Leto, P., & Antiochos, S. K. 1994, ApJ, 427, 453
Spitzer, L. 1962, Physics of Fully Ionized Gases (Physics of Fully Ionized Gases, New York: Interscience (2nd edition), 1962)
Suleiman, R. M., Crooker, N. U., Raymond, J. C., & van Ballegooijen, A. 2005, in IAU Symposium, Vol. 226, Coronal and Stellar Mass Ejections, ed. K. Dere, J. Wang, & Y. Yan, 71–75
Webb, D. F., Cliver, E. W., Crooker, N. U., Cry, O. C. S., & Thompson, B. J. 2000, J. Geophys. Res., 105, 7491
Zhang, J., Dere, K. P., Howard, R. A., & Bothmer, V. 2003, ApJ, 582, 520